A Polymorphic Residue That Attenuates Interferon Lambda 4 Activity in Hominid Lineages

Connor G. G. Bamford[1], Elihu Aranday-Cortes[1], Inès Cordeiro Filipe[1], Swathi Sukumar[1], Daniel Mair[1], Ana da Silva Filipe[1], Juan L. Mendoza[2], K. Christopher Garcia[2], Shaohua Fan[3], Sarah A. Tishkoff[3], John McLauchlan[1,4]

[1]MRC-University of Glasgow Centre for Virus Research, Glasgow G61 1QH, UK

[2]Howard Hughes Medical Institute, Department of Molecular and Cellular Physiology and Department of Structural Biology, Stanford University School of Medicine, Stanford, CA 94305, USA

[3]Departments of Genetics and Biology, University of Pennsylvania, Philadelphia PA19104-6145, USA

[4]Corresponding Author/Lead Contact: John McLauchlan; john.mclauchlan@glasgow.ac.uk

Word Count: 2,500

SUMMARY

Type III or lambda interferons (IFNλs) form a critical barrier to infection by diverse pathogens. However in humans, production of IFNλ4 is associated with decreased clearance of hepatitis C virus (HCV). How an antiviral cytokine came to promote infection and whether this phenomenon occurs in other species is unknown. Here we show that, compared to chimpanzee IFNλ4, the human orthologue has reduced activity due to a single amino acid substitution (E154K). IFNλ4s with E154 restrict virus infection more potently and induce more robust antiviral gene expression. Remarkably, E154 is the ancestral residue in mammalian IFNλ4s but altered in representatives of the *Homo* genus. Nonetheless, the more active E154 form of IFNλ4 can be found in African Congo rainforest 'Pygmy' hunter-gatherers. We postulate that evolution of an IFNλ4 with attenuated activity in humans has been exploited by pathogens such as HCV, which could explain distinct host-specific outcomes of infection.

KEYWORDS

Hepatitis C virus, interferon, evolution, interferon lambda 4, interferon-stimulated genes, antiviral activity.

MAIN TEXT

Vertebrates co-ordinate antiviral defences through the action of signalling proteins called interferons (IFNs). IFNs induce expression of hundreds of 'interferon-stimulated genes' (ISGs), which establish a cell-intrinsic 'antiviral state' and regulate inflammation (Randall and Goodbourn 2008). Thus, IFNs are pleiotropic in activity and modulate aspects of protective immunity and pathogenesis (Schoggins 2014). Three groups of IFNs have been identified (types I – III), with the type III family – or IFNλs - being the most recently discovered (reviewed in Lazear et al. 2015b). Emerging evidence highlights the critical and non-redundant role IFNλs play in protecting against diverse pathogens, including viruses, bacteria, and fungi (Dixit et al. 2010, Nice et al. 2015, Lazear et al. 2015a, Galani et al. 2017, Odendall et al. 2017, Espinosa et al. 2017).

Although important in host defence, some IFNs are highly polymorphic (Manry et al. 2011). A single nucleotide insertion converting the 'ΔG' allele to a 'TT' allele (rs368234815) yields a frameshift leading to loss of active human IFNλ4 (HsIFNλ4) (Prokunina-Olsson et al. 2013). Although IFNλ4 is highly conserved among mammals, the TT allele has evolved under positive selection in some human populations (Key et al. 2014). Despite their broad antimicrobial functions, genome-wide association studies have convincingly demonstrated a correlation between ΔG IFNλ4 and reduced spontaneous clearance of hepatitis C virus (HCV) infection, i.e individuals homozygous for TT clear HCV infection with greater frequency (Ge et al. 2009, Prokunina-Olsson et al. 2013). HsIFNL4 has also been linked to protection from liver inflammation (Eslam et al. 2015) and reduced HCV treatment response (Prokunina-Olsson et al. 2013). The mechanism underlying this contribution of HsIFNλ4 to viral persistence and pathogenesis is not well understood but is associated with differences in ISG induction (Terczyńska-Dyla et al. 2014).

A major remaining question is how *IFNL4* evolution has led to it occupying a 'pro-viral' role during HCV infection. To address this question, we explored whether differences in IFNλ4-mediated antiviral signalling exist between closely-related host species (humans versus chimpanzees, *Pan troglodytes*) in response to a common pathogen (HCV), taking advantage of the historical use of experimental infection of chimpanzees.

To this end, we compared intrahepatic gene expression during early HCV infection in humans and chimpanzees using published transcriptomic data (see Experimental Procedures). This revealed distinct host responses in humans and chimpanzees as well as overlapping differentially-regulated genes (Figure 1A and Supplementary Data File 1). In chimpanzees, the transcriptional profile was dominated by ISGs known to restrict HCV infection (*RSAD2, IFI27* and *IFIT1*) (Schoggins et al. 2011), as well as genes involved in antigen presentation and adaptive immunity (*HLA-DMA* and *PSMB8*). These genes were not significantly differentially expressed in humans, whose response was mainly directed towards up-regulation of pro-inflammatory genes (for example*, CXCL10, CCL18* and *CCL5*) (Figures 1A and 1B). 'Chimpanzee-specific' differentially-expressed genes were induced early in infection and remained significantly up-regulated during the acute phase (Figure 1B). We hypothesised that the more robust antiviral response to HCV infection in chimpanzees compared to humans could arise from host genetic differences.

Given the marked up-regulation of antiviral ISGs during acute infection in chimpanzees and relevance of IFNλ4 during HCV infection in humans, we undertook genetic and functional comparisons of natural human IFNλ4 coding variants and between human and chimpanzee *IFNL4* orthologues. In humans, we identified 15 non-synonymous HsIFNλ4 variants in the

1000 Genomes Project database (Figure S1A and Supplementary Data File 2), including the only three previously described variants (C17Y, P60R and P70S; >1% frequency, 'common') (Prokunina-Olsson et al. 2013). The remaining 12 variants were classified as rare (<1% frequency). Variants were located in functional regions such as the predicted signal peptide (amino acids 1-24), surrounding the single glycosylation site (N61), and helix F that interacts with the *IFNλR1* receptor (variants 151–158; Figure 1C)**.** The chimpanzee *IFNL4* gene (encoding PtIFNλ4) differs from the human orthologue at six amino acid (aa) positions (data not shown). However, only one, aa154, differed both within humans and between species.

Screening the entire panel of HsIFNλ4 variants in antiviral (EMCV, which is a highly IFN-sensitive virus [Figure 1D]) and ISG mRNA induction assays (*MX1*, Figure S1B and *ISG15*, data not shown) revealed three out of 15 variants substantially affected activity. Consistent with previous data (Terczyńska-Dyla et al. 2014), P70S had reduced activity; a similar decrease in activity was also observed for L79F. By contrast, K154E enhanced antiviral activity by ~10-fold. These effects on activity did not arise from differences in the levels of HsIFNλ4 production or glycosylation (Figures S1C and S1D) and for K154E, enhanced secretion could not explain its higher activity (Figure S1E).

Remarkably, glutamic acid (E) is encoded at position 154 in most mammals with an *IFNL4* orthologue, including chimpanzees (Figure 1E). Therefore, we compared wt HsIFNλ4 and its K154E variant to wt PtIFNλ4 and an equivalent 'humanised' E154K mutant in functional assays. wt PtIFNλ4 was significantly more active than HsIFNλ4 in each assay and had approximately equivalent potency to the HsIFNλ4 K154E variant (Figures 1F-1H). Moreover, PtIFNλ4 E154K had decreased activity similar to wt HsIFNλ4 (encoding lysine at aa154). Extending the analysis to include rhesus macaque IFNλ4 (*Macaca mulatta*,

MmIFNλ4) gave the same pattern whereby wt MmIFNλ4 with E154 had greater activity than its K154 variant. By contrast, introducing a lysine into HsIFNλ3 had less of an effect on its activity (Figure 1F to H). Thus, we conclude that HsIFNλ4 has weaker activity compared to primate orthologues principally because of a single amino acid change at position 154.

We next examined the impact of HsIFNλ4 K154E on HCV infection *in vitro* as well as infectious assays with influenza A virus (IAV) and Zika virus (ZIKV). We also included the less active P70S and L79F HsIFNλ4 variants in these assays. Using the HCVcc infectious system, HsIFNλ4 K154E decreased both viral RNA abundance (Figure 2A) and the number of infected cells (Figure S2A), whereas P70S and L79F were less active than wt HsIFNλ4. To determine the stage in the HCV life cycle targeted by K154E, we performed assays examining virus entry (HCV pseudoparticle system [HCVpp]), initial viral RNA translation and RNA replication (both assessed by the HCV sub-genomic replicon). HsIFNλ4 K154E did not significantly alter HCVpp entry or translation of replicon RNA compared to wt protein whereas HCV RNA replication was significantly reduced by the K154E variant (Figure 2B and Figure S2B and C). HsIFNλ4 K154E also reduced titers of IAV and ZIKV to a greater extent than wt protein (Figure S2D and S2E). Correspondingly, the P70S and L79F HsIFNλ4 variants were less active than wt protein.

To examine effects of HsIFNλ4 on global transcription, cells were stimulated with HsIFNλ4s and their transcriptomes analysed, which revealed that K154E induced the broadest profile of up-regulated genes (n = 149) compared with either the wt protein (n = 88) or the P70S variant (n = 71; Figures 2D/E and S2F/G). Many of the shared differentially-expressed genes included known restriction factors (*IFI27, MX1, ISG15*), and several unique K154E ISGs with antiviral activity, such as *IDO1* and *ISG20,* alongside signalling activators such as

STING and *IRF1*. From pathway analysis, all HsIFNλs induced similar transcriptional programmes with differences in the overall significance of these pathways, most notably enhancement of the antigen presentation and protein ubiquitination pathways with K154E (Figure S2H). The majority (20/32) of the chimpanzee-specific differentially-regulated genes (Figures 1A and B) were induced by HsIFNλ4 stimulation, with approximately half of those being significantly up-regulated with K154E compared to wt, including *MX1*, *IFITM1*, *IFIT1* and *IFIT3*, *TRIM22* and *IFI44L* (Figure 2F). Together, these data show that similar to PtIFNλ4, the HsIFNλ4 K154E, which is rarely found in humans, has greater activity and antiviral potential compared to the wt protein that is common in the human population.

From further interrogation of human genome datasets (Lachance et al. 2012), the rare HsIFNλ4 K154E variant was present in two individuals from different African rainforest 'Pygmy' hunter-gatherer populations (Baka and Bakola) in Cameroon (Figure 2G). The Bakola individual was homozygous for the ΔG allele, indicating that the K154E variant can give rise to functional HsIFNλ4. The Baka subject was heterozygous at rs368234815 (ΔG/TT) and thus could produce either wt or the more active K154E form of HsIFNλ4. Each of these individuals also had additional non-synonymous HsIFNλ4 variants (V158I and R151P, Baka and Bakola individuals respectively); these variants were included in our functional screen of HsIFNλ4 variants but did not significantly alter activity (Figures 1D and S1B). K154E was not found in other African hunter-gatherer populations (such as Hadza and Sandawe, Figure 2H) nor in the African San, who have the oldest genetic lineages among humans, nor was it identified in Neanderthal and Denisovan. Notably, the human TT allele encodes a K154 codon (data not shown) suggesting that the less active E154K substitution emerged very early during human evolution but not in chimpanzees, our closest living relative.

For decades, experimental studies in chimpanzees have provided unique insight into human HCV infection (Bukh 2004) but chimpanzees do not present with identical clinical outcomes. For example, chimpanzees may clear infection more efficiently (Bassett et al., 1998), rarely develop hepatic diseases similar to humans (Walker 1997) and are refractory to IFNα therapy (Lanford et al. 2007). Moreover, HCV evolves more slowly in chimpanzees, possibly due to stronger immune pressure that reduces replication (Ray et al. 2000). We propose that the enhanced activity observed with PtIFNλ4 contributes to the distinct chimpanzee response to HCV infection.

Acute HCV infection in humans and chimpanzees (and human hepatocytes *in vitro*) selectively stimulates type III over type I IFN production (Park et al. 2012, Thomas et al. 2012). A heightening of the IFN response to HCV has been postulated to explain the capacity to control HCV infection (Sheahan et al. 2014, Boldanova et al. 2017). Enhanced expression of ISGs in chimpanzees due to higher IFNλ4 activity could lead to greater inhibition of viral infection by coordinating a more efficient adaptive immune response, which is critical for clearance and disease (Thimme et al. 2002). We observed enhanced expression of genes involved in antigen presentation and T cell mediated immunity alongside HCV restriction factors in chimpanzees compared to humans and in IFNλ4 K154E stimulation *in vitro*. Additionally, IFNλ4 can inhibit type I IFN signalling (Fan et al. 2016) and inflammation (Blazek et al. 2015). Therefore, IFNλ4 with enhanced activity may act as a core co-ordinator of both protective innate and adaptive immunity.

Based on available IFNλ1 and IFNλ3 crystal structures (Miknis et al. 2010, Mendoza et al. 2017), the equivalent position to aa154 in IFNλ4 is located on the IFNλ receptor (R) 1-

binding helix F, although the glutamic acid side chain faces inward towards the opposing IL10R2-binding helices (A and D; Figure 2I). This position forms non-covalent intramolecular interactions with two regions (residues K64/K67 and T108 [IFNλ3 only]) mediated by the free carboxyl group of glutamic acid. In IFNλ4, the E154-interacting positions are not conserved with IFNλ1/3 but biochemically homologous positions exist (e.g R60 and R98). We propose that E154K prohibits these critical interactions, reducing HsIFNλ4 activity via affecting receptor binding. Our data support a direct role on protein activity rather than altered production or secretion. Additionally, modelling of L79F showed that leucine sits internally and that replacement with phenylalanine would likely disrupt packing of the helices (Figure S2I).

In humans, the E154 variant was found only in African rainforest 'Pygmy' hunter-gatherers from west central Africa (Lachance et al. 2012). A recent study in Pygmies from Cameroon, including the Baka and Bakola groups, showed low seroprevalence of 0.6% and no evidence of chronic HCV infection (Foupouapouognigni et al. 2011). By contrast, infection in other groups in Cameroon has a seroprevalence of ~17% (Njouom et al. 2003). One explanation for this difference is higher IFNλ4 activity in populations with the K154E variant, which would enhance HCV clearance and lower endemic transmission. As San and Neanderthal and Denisovan lacked E154, Pygmy populations likely re-acquired it rather than retaining it following divergence of chimpanzee and humans. The factors driving divergent evolution of IFNλ4 within and between species are not known but we speculate that different microbial burdens might play a role, such as exposure to highly-pathogenic zoonotic infections in the Congo rainforest (Mulangu et al. 2016), a habitat shared by Pygmies and chimpanzees.

Our data beg the question as to why the vast majority of humans do not encode the more active E154 variant. We propose that it is likely that the apparent selective disadvantage the

less active IFNλ4 K154 allele confers in the face of HCV infection is counterbalanced by selective advantages in other contexts. For example, type III IFN signalling has been shown to enhance disease and impede bacterial clearance in mouse models of bacterial pneumonia (Cohen et al. 2013), suggesting that IFNλ4 with a lower activity could be beneficial during non-viral infections. To conclude, our study supports a significant and non-redundant role for IFNλ4 in controlling immunity whose activity has been repeatedly attenuated during human evolution, commencing with E154K.

AUTHOR CONTRIBUTIONS

CGGB, EAC and JMcL designed the experiments. CGGB, EAC, ICF, SS and DM conducted the experiments. CGGB, EAC, SS, AdSF, JLM, KCG, SF and ST provided and analyzed data. CGGB and JMcL composed the manuscript. All authors critically reviewed the manuscript.

ACKNOWLEDGEMENTS

We are grateful to: Chris Boutell and Prof Alain Kohl for IAV and ZIKV respectively; Takaji Wakita, Ralf Bartenschlager and Arvind Patel for HCV reagents; Sam Wilson and Carol McWilliam Leitch for critically reading the manuscript. SF and ST were supported by NIH grants 1R01DK104339-0 and 1R01GM113657-01. This work was funded by the UK Medical Research Council (MC_UU_12014/1).

EXPERIMENTAL PROCEDURES

Comparison of human and chimpanzee intrahepatic gene expression during acute HCV infection

Previously published datasets of intrahepatic differentially-expressed genes from liver biopsies were used to compare human and chimpanzee transcriptomic responses to early HCV infection. Studies focusing on acute HCV infection (0 to 26 weeks) in humans and chimpanzees were acquired through manual literature search using Pubmed and compiled. For chimpanzees, data was acquired from 4 studies (Bigger et al. 2001, Su et al. 2002, Nanda et al. 2008, Yu et al. 2010) and one report was employed for human data (Dill et al. 2012). The study by Dill et al. comprised single biopsy samples from each of six individuals, while *in toto* the chimpanzee studies combined data from ten animals with multiple, serial biopsies. All studies were carried out using similar Affymetrix microarray platforms except Nanda et al. who used IMAGE clone deposited arrays. Humans were infected with HCV genotype (gt)1 (n = 2), gt3 (n = 3) and gt4 (n = 1) while chimpanzees were experimentally infected with HCV gt1a (n = 6), gt1b (n = 3) and gt2a (n = 1). Gene names and fold-changes were manually converted to a single format (fold change rather than log2 fold change for example) to allow comparative analysis. Human biopsies were taken between two and five months after presumed infection following known needle-stick exposure, and serial chimpanzee biopsies were taken at different time points from between one week and one year following HCV infection. For comparative purposes, differentially-expressed genes in chimpanzees were included if they were detected during a time period overlapping with the human data. We identified a 'core' set of chimpanzee differentially-expressed genes (independently characterized in at least two studies) and compared them to the single human transcriptome study data at equivalent time points (between 8 and 20 weeks post-infection). This approach generated a set of core chimpanzee genes (genes found differentially-expressed in at least 2

studies, >2 fold change compared to controls and during the time frame compared to humans) for comparison with the human data. This is reflected in the ten-fold higher numbers of differentially-regulated genes found in the one human study compared to the 'core' (narrowed down) set assembled from four chimpanzee studies. These gene sets were compared to determine their degree of species-specificity or species-similarity using Venn diagram analysis (http://bioinfogp.cnb.csic.es/tools/venny/). The gene lists of humans and core genes for chimpanzees are shown in the Supplementary Data File 1. For the chimpanzee-specific genes, mean expression values were determined at each time point from individual animals.

IFNλ gene sequence analysis

Complete known human *IFNL4* genetic variation along with associated frequency and ethnicity for the human population were collected from the 1000 Genomes database available at the time of study (June 2016) (http://browser.1000genomes.org/index.html). The reference sequence for the human genome contains the frameshift 'TT' allele and so potential effects of variants on the HsIFNλ4 predicted amino acid sequence were identified manually following correction for the frameshift mutation (TT to ΔG). The effect of all single nucleotide polymorphisms (SNPs) on the open reading frame (ORF) was thus assessed and re-annotated as synonymous or non-synonymous resulting in the selection of coding variants reported here. Inspection of whole genome sequence data from African hunter-gatherers was carried out using previously published datasets (Lachance et al. 2012). We remapped the raw reads of six San individuals (four Ju|'hoan and two ‡Khomani San) in the Simon Genomic Diversity Project (Mallick et al. 2016) to human reference genome (hg19) and conducted variant calling using the haplotype caller module in GATK (v3). Two Ju|'hoan individuals were heterozygous at rs368234815 (TT/ΔG genotype, Supplementary Data File 2). The

genotypes of rs368234815 in Neanderthal and Denisovan were extracted from VCF files that were downloaded from http://cdna.eva.mpg.de/denisova/VCF/hg19_1000g/ and http://cdna.eva.mpg.de/neandertal/altai/AltaiNeandertal/VCF/. Neanderthal and Denisovan all contained only ΔG alleles (Supplementary Data File 2). Amino acid sequences for mammalian IFNλ genes were obtained from NCBI following protein BLAST of the wt HsIFNλ4 polypeptide sequence. Multiple alignments of IFNλ amino acid sequences were performed by MUSCLE using MEGA7. Accession numbers of specific IFNλs used in the experimental section of this study were as follows: HsIFNλ3: Q8IU54; HsIFNλ3, Q8IZI9.2; and for IFNλ4: *Homo sapiens* AFQ38559.1; *Pan troglodytes* AFY99109.1; *Macaca mullata* XP_014979310.1; *Pongo abelii* (orangutan) XP_009230852.1, *Bos* taurus (cow) XP_005219183.1, *Felis catus* (cat) XP_011288250.1.

Structural modelling

A homology model of the HsIFNλ4 structure was generated using the RaptorX online server (http://raptorx.uchicago.edu). The resultant HsIFNλ4 structural model was then structurally aligned with both HsIFNλ1 (PDB 3OG6) (Miknis et al. 2010) and HsIFNλ3 (PDB 5T5W) (Mendoza et al. 2017). Visualization, structural alignments, and figures were generated in Pymol (The PyMOL Molecular Graphics System, Version 1.8).

Recombinant DNA manipulation and generation of IFNλ expression plasmids

DNA sequences encoding the ORFs of HsIFNλ4, PtIFNλ4 and MmIFNλ4 (based on accession sequences above) were synthesized commercially with a carboxy-terminal DYKDDDDK/FLAG tag using GeneStrings or Gene Synthesis technology (GeneArt). As a positive control for functional assays, the HsIFNλ3 ORF was codon optimised (human) to ensure robust expression and antiviral activity and is termed 'HsIFNλ3op'. All IFNλ4 coding

region sequences were retained as the original nucleotide sequence without optimisation. This precluded a direct functional comparison of HsIFNλ3op and wt HsIFNλ4. Synthesized DNA was cloned into mammalian expression vectors (pCI, Promega) using standard molecular biology techniques. At each cloning step, the complete ORF was sequenced to ensure no spurious mutations had occurred during plasmid generation and manipulation. Single amino acid changes were incorporated using standard site-directed mutagenesis protocols (QuickChange site-directed mutagenesis kit [Agilent], or using overlapping oligonucleotides and Phusion PCR).

Cell lines

A549 (human lung adenocarcinoma), Huh7 (human hepatoma), HEK293T (human embryonic kidney), U2OS (human osteosarcoma), Vero (African Green Monkey kidney) and MDCK (Madin-Darby canine kidney) cells were grown in DMEM growth media supplemented with 10% FBS and 1% penicillin-streptomycin. Non-differentiated human hepatic progenitor HepaRG cells and derivatives were cultured in William's E medium supplemented with 10% of FBS, 1% penicillin-streptomycin, hydrocortisone hemisuccinate (50 µM) and human insulin (4 µg/mL). All cells were grown at 37°C with 5% CO_2.

Plasmid transfection and production of functional IFNλ

Plasmid DNA generated by midiprep of bacterial cultures (GeneJET plasmid midiprep kit, ThermoScientific) was introduced into cells by lipid-based transfection using Lipofectamine 2000 or Lipofectamine 3000 (ThermoFisher) following manufacturer's instructions. To produce IFN-containing conditioned media (CM) or measure protein production, HEK293T 'producer' cells were grown to near-confluency in 12 (~4 x 10^5 cells

per well) or 6-well (~1.2 x 10^6 cells per well) plates and transfected with plasmids (2 μg) in OptiMEM (1-2 mL) overnight. At approximately 16 hours (hrs) post transfection (hpt), OptiMEM was removed and replaced with complete growth media (1-2 mL). CM containing the extracellular IFNλs was harvested at 48 hpt and stored at -20ºC before use. Although antiviral activity was observed at 16 hpt, we chose 48 hpt to harvest CM to ensure robust production and secretion of each IFNλ. Intracellular IFNλs also were harvested from transfected cells at 48 hpt. CM was removed and replaced with fresh DMEM 10% FCS (2 mL) and then frozen at -70ºC. To prepare cell lysates with IFNλ activity, plates were thawed and the cell monolayer was scraped into the media and clarified by centrifugation (5 minutes [mins] x 300 g) before use. CM or lysates were diluted in the respective growth medium for each cell line before functional testing as described in the text.

Relative quantification of RNA by reverse transcriptase-quantitative polymerase chain reaction (RT-qPCR)

Total cellular RNA was isolated by a column-based guanidine thiocyanate extraction using RNeasy Plus Mini kit (genomic DNA removal 'plus' kit, Qiagen) and following the supplier's protocol. cDNA was synthesised by reverse transcribing RNA (1 μg) using random primers and the AccuScript High Fidelity Reverse Transcriptase kit (Agilent Technologies); the recommended protocol was followed. Relative expression of mRNA was quantified by qPCR (7500 Real-Time PCR System, Applied Biosystems) of amplified cDNA. Probes for *ISG15* (Hs01921425), *Mx1* (Hs00895608) and the control *GAPDH* (402869) were used with TaqMan Fast Universal PCR Master Mix (Applied Biosystems). The results were normalised to *GAPDH* and presented in $2^{-\Delta\Delta Ct}$ values relative to controls as described in the text. HCV genomic RNA was quantified by RT-qPCR as described previously (Jones et al. 2010).

Global transcriptomic measurements and corresponding pathway analysis

IFN-competent cells (A549) were stimulated with IFN CM (1:4 dilution) in 6-well plates (~1.2 x 10^6 cells) for 24 hrs and global gene expression was assessed by RNA-Seq, using three biological replicates per condition. Sample RNA concentration was measured with a Qubit Fluorometer (Life Technologies) and RNA integrity was determined using an Agilent 4200 TapeStation. All samples had a RNA integrity number of 9 or above. 1.5 μg of total RNA from each sample was prepared for sequencing using an Illumina TruSeq Stranded mRNA HT kit according to the manufacturer's instructions. Briefly, polyadenylated RNA molecules were captured, followed by fragmentation. RNA fragments were reverse transcribed and converted to dsDNA, end repaired, A-tailed, ligated to indexed adaptors and amplified by PCR. Libraries were pooled in equimolar concentrations and sequenced in an Illumina NextSeq 500 sequencer using a high output cartridge, generating approximately 25 million reads per sample, with a read length of 75 bp. 96.3% of the reads with Q score of 30 or above. Data was demultiplexed and fastq files were generated on a bio-linux server using bcl2fastq version v2.16. RNA-Seq analysis was performed using the Tuxedo protocol (Trapnell et al. 2012). Differential gene expression was considered significant when the observed fold change was ≥2.0 and FDR/q-value was <0.05 between comparisons. Pathway analysis was carried out using Ingenuity Pathway Analysis [IPA] (Ingenuity Systems, Redwood City, CA, USA).

Western blot analysis

Cell growth media was removed and monolayers were rinsed once with approximately 0.5mL PBS before lysis using RIPA buffer (ThermoFisher) containing protease inhibitor cocktail (1x Halt Protease inhibitor cocktail, ThermoFisher, or cOmplete™, Mini, EDTA-free Protease Inhibitor Cocktail, Sigma Aldrich) for 10 mins at 4ºC before being frozen at -20 ºC

overnight. Lysates were collected into a 1.5 mL sample tube and clarified by centrifugation (max speed for 15 mins). Samples (10 µl) from the soluble fraction were heated to 90ºC for 10 mins with 100 mM dithiothreitol (DTT)-containing reducing lane marker at 90ºC for 10 mins. Samples were run on home-made 12% SDS-PAGE gels alongside molecular weight markers (Pierce Lane marker, Thermofisher) before wet-transfer to a nitrocellulose membrane. Membranes were blocked using a solution of 50% PBS and 50% FBS for 1 hour at room temperature and then incubated overnight at 4^{o}C with primary antibodies in 50% PBS, 50% FBS and 0.1% TWEEN 20. Secondary antibodies were incubated in 50% PBS, 50% FBS and 0.1% TWEEN for 1 hour at room temperature. Membranes were washed four times (5 mins each) following each antibody incubation with PBS containing 0.1% TWEEN 20. After the 4th wash following incubation with the secondary antibody, the membrane was washed once more in PBS (5 mins) and kept in dd$H_2$0 until imaging. Primary antibodies to the FLAG tag (1:1000) (rabbit, lot. 064M4757V) and α-tubulin (1:10000) (mouse, lot. GR252006-1) were used along with infra-red secondary antibodies (LI-COR) to anti-rabbit (donkey [1:10,000], 926-68073) and anti-mouse (donkey [1:10,000], C50422-05) to allow protein visualisation. Pre-stained, Pagerule Plus marker was used to determine molecular weights (ThermoFisher). Membranes were visualised using the LI-COR system on an Odyssey CLX and the relative expression level of proteins determined using LI-COR software (Image Studio).

Generation and use of IFN reporter cell lines

An IFN reporter HepaRG cell line was generated to measure the activity of IFNs by introducing the EGFP ORF fused to the ISG15 ORF separated by ribosome skipping sites by CRISPR/Cas9 genome editing. We chose to introduce EGFP in-frame to the N-terminus of the *ISG15* ORF because it is a robustly-induced ISG. To facilitate this we also introduced

the blasticidin resistance gene (BSD). BSD, EGFP and ISG15 were separated using ribosome skipping 2A sequences (P2A and T2A). Transgene DNA was flanked by homology arms with reference to the predicted target site. Homology donor plasmids for CRISPR/Cas9 knock-in were generated through a series of overlapping PCR amplifications using Phusion DNA polymerase followed by sub-cloning into pJET plasmid. Plasmids for CRISPR/Cas9 genome editing (wt SpCas9) were generated using established protocols (Ran et al. 2013) in order to generate plasmids that would direct genome editing at the 5' terminus of the HsISG15 ORF (exon 2). pSpCas9(BB)-2A-Puro (PX459) V2.0 was a gift from Feng Zhang (Addgene plasmid # 62988). All sequences are available by request. HepaRG cells grown in 6 well dishes were co-transfected with CRISPR/Cas9 editing plasmids targeting the beginning of the ISG15 ORF in exon 2 (exon 1 contains only the ATG of the ORF), and homology donor plasmids described above (1 µg each) using Lipofectamine 2000 and the protocol described above. Transfected cells were selected using puromycin (Life Technologies) (1 µg/mL) and blastocidin (Invivogen) (10 µg/mL) until non-transfected cells were no longer viable. Selected cells were cloned by single cell dilution, expanded and tested for EGFP induction following IFN stimulation. Positioning of the introduced transgene was assessed by PCR amplification on isolated genomic DNA from individual clones (data not shown). Primers were designed to include one primer internal to the transgene and another external to the transgene and found in the target loci (sequences available on request). For use as an effective IFN reporter cell line, cells had to demonstrate robust induction of EGFP expression following stimulation with IFN and have evidence of specific introduction of the transgene. This study uses clone 'G8' of HepaRG.EGFP-BSD-ISG15 cells. However, we have not tested whether there is a single transgene integration site or multiple ones nor confirmed that the EGFP produced following stimulation by IFNs results from the expression of the specifically-introduced transgene rather than off-target integration, which is

433 theoretically possible. However, we do not predict this would affect the cells' ability to act as
434 a reporter cell line. For use in IFN reporter assays, stimulated cells (in 96 well plates
435 stimulated for 24 hrs; ~5 x 10^4 cells per well) were washed, trypsinised and fixed in formalin
436 (1% in PBS) at room temperature for 10 mins in the dark before being transferred to a round-
437 bottomed plate and stored at 4^{o}C in the dark until measurement. Non-stimulated cells were
438 used as negative controls and the change in % EGFP-positive cells was assessed by flow
439 cytometry using a Guava easyCyte HT (Merck Millipore).
440
441 **Production of virus stocks for antiviral assays**
442 Antiviral activity of IFNλs was determined using encephalomyocarditis virus (EMCV),
443 influenza A virus (IAV; A/WSN/1933(H1N1)), Zika virus (ZIKV; Brazilian strain PE243)
444 (Donald et al. 2016) and HCV (HCVcc chimeric clone Jc1) (Pietschmann et al. 2006).
445 EMCV was obtained from and amplified on Vero cells and titrated on U2OS cells by plaque
446 assay. IAV stocks were generated on MDCK cells and titrated by plaque assay on MDCK
447 cells with protease (TPCK-treated trypsin, Sigma Aldrich). ZIKV was titrated on Vero cells
448 by plaque assay. For all plaque assays, cells were grown in 12 or 6-well plates to ~90%
449 confluency before inoculation with serial ten-fold dilutions of virus stocks in serum-free
450 Optimem. Inoculum remained on the cells for two hrs before being removed and the
451 monolayers were rinsed with PBS (1 x) and semi-solid Avicell overlay (Sigma Aldrich) was
452 added. For EMCV and IAV, 1.2% avicell was used, diluted in 1X DMEM 10% FCS, 1%
453 penicillin-streptomycin. For IAV titration, TPCK-treated trypsin was added (1 μg/mL). For
454 ZIKV plaque assay, 2X MEM was used instead of 1X DMEM. HCVcc Jc1 was generated as
455 described previously by electroporation of *in vitro* transcribed RNA into Huh7 cells and
456 harvested at 72 hrs post electroporation. After filtration of the supernatant, HCVcc Jc1 stocks
457 were titrated by $TCID_{50}$ on Huh7 cells and stored at 4^{o}C before use. HCVcc Jc1 $TCID_{50}$

458 assays were performed using anti-NS5A antibody (Lindenbach et al. 2005). Infected cells at
459 72 hrs post infection were fixed and permeabilised with ice-cold methanol. Cells were rinsed
460 in PBS, blocked with FCS at room temperature, incubated overnight with mouse monoclonal
461 anti-NS5A antibody (9E10) at 4^{o}C. After removal of the antisera, cells were rinsed 3 times
462 with PBS containing 0.1% TWEEN 20, and then incubated in the dark at room temperature
463 for 1 hour with secondary antibody [Alexa-fluor 488nm anti-mouse (donkey)]. Cells were
464 finally washed with PBS containing 0.1% TWEEN 20 and NS5A-expressing cells were
465 visualized with a fluorescent microscope.
466
467 **Antiviral assays**
468 Cells stimulated with IFNs were infected with viruses at the following multiplicities of
469 infection (MOI): EMCV (MOI = 0.3; added directly to the media); IAV (MOI = 0.01); ZIKV
470 (MOI = 0.01); HCVcc (MOI = 0.05). For IAV, ZIKV and HCVcc, the inoculum was
471 incubated with cells for at two (IAV/ZIKV) or three hrs (HCVcc) in 0.5–1.0 mL serum-free
472 Opti-MEM/DMEM at 37^{o}C before removal. Cells were rinsed with PBS and then incubated
473 with fresh growth media for the allotted time (24 hrs for EMCV, 48 hrs for IAV and 72 hrs
474 for ZIKV and HCVcc). At the times stated for individual experiments, infected-cell
475 supernatants were harvested and infectivity was titrated by plaque assay. IAV, ZIKV and
476 HCVcc antiviral assays were all carried out in 12 well plates except for measurement of
477 HCVcc infectivity by indirect immunofluorescence, which was measured in a 96 well plate.
478 In the case of EMCV, a cytopathic effect (CPE) protection assay was employed to assess
479 infectivity (Mohamed et al. 2009). Here, HepaRG cells were plated in a 96-well plates (~5 x
480 10^4 cells per well) and, when confluent, were incubated with two-fold serial dilutions of CM
481 or lysate for 24 hrs before the addition of EMCV. At 24 hrs post infection with EMCV media
482 was removed; cell monolayers were rinsed in PBS and stained using crystal violet (1% in

20% ethanol in H_20) for 10 mins. Crystal violet stain was then removed and stained plates were washed in water. The dilution of ~50% inhibition of EMCV-induced CPE was marked visually and the difference determined relative to wt HsIFNL4.

Luciferase-expressing MLV pseudoparticles with (JFH1 HCV E1E2) were generated as described (Cowton et al. 2016) along with their corresponding E1E2 deficient controls (particles generated only with MLV core) and used to challenge IFN-stimulated Huh7 cells. Huh7 cells grown in 96-well plates overnight (seeded at 4 x 10^3 cells per well) were stimulated with IFNs for 24 hrs and transduced with HCVpp. 72 hrs later, cell lysates were harvested and luciferase activity was measured (Luciferase assay system, Promega) on a plate reading luminometer.

For HCV RNA replication assays, RNA was transcribed *in vitro* from a sub-genomic replicon (HCV-SGR) expressing GLuc (wild-type and non-replicating GND) (Domingues et al. 2015). *In vitro* transcribed RNA (200 ng) was transfected using PEI (1:1) into monolayers of Huh7 cells in 96-well plates overnight (seeded at 4 x 10^3 cells per well) that had been stimulated with IFNs (24 hrs). At the specified time points, total supernatants (containing the secreted GLuc) from treated Huh7 cells were collected and replaced with fresh growth media. 20µL (~10% of total volume) was used to measure luciferase activity and mixed with GLuc substrate (1x) (50 µL) and luminescence (as relative light units, RLUs) was determined using a luminometer (Promega GloMax). Pierce *Gaussia* Luciferase Flash Assay Kit (ThermoFisher) was used and the manufacturer's instructions were followed.

Statistical analysis

For non-transcriptomic analysis (outlined above), Graphpad Prism was used for statistical testing, which included Students' T test and ANOVA as described in figure legends. *** = <0.001; ** = <0.01; * = <0.05, are used throughout to denote statistical significance.

FIGURE LEGENDS

Figure 1. Human IFNλ4 is less active than chimpanzee IFNλ4

A) Numbers of shared and unique differentially-expressed genes in liver biopsies from HCV-infected humans (blue) and experimentally-infected chimpanzees (orange) during the acute phase of infection represented as a Venn diagram (also see Supplementary Data File 1). Gene expression during a time period of between 8 and 20 weeks was used where comparable published data for both species exists. The top ten species-specific, differentially-expressed genes are shown ranked by levels of expression.

B) Expression of 'chimpanzee-specific' differentially-expressed genes over time (n = 32). Chimpanzee-specific genes are shown as a combined mean (orange line) and range (grey lines) of fold-change from all studies where any gene of the 32 genes was available over at most ~1 year of infection. The time period of 8 to 20 weeks that overlaps with the equivalent human genes which are differentially expressed is boxed (blue); at this time the 32 genes were not observed in human datasets.

C) Location of non-synonymous variants in the HsIFNλ4 polypeptide (underlined pink). Regions of predicted structural significance are boxed (green), including the signal peptide (sp) and helices (A to F) (Hamming et al. 2013). Note that there are 2 non-synonymous changes at C17 (C17R and C17Y). See Supplementary Data File 2 for genetic identifiers for SNPs described here.

D) Antiviral activity of all HsIFNλ4 natural variants and wt in an anti-EMCV CPE assay relative to wt protein in HepaRG cells. Cells were stimulated with serial dilutions of HsIFNλ4-containing conditioned media (CM) for 24 hrs and then infected with EMCV (MOI = 0.3 PFU/cell) for 24 hrs at which point CPE was assessed by crystal

violet staining. After staining, the dilution providing ~50% protection was determined. Variants HsIFNλ4 P70S (blue), HsIFNλ4 L79F (yellow) and HsIFNλ4 K154E (purple) have the greatest effect on antiviral activity (>2-fold and significant: ** for P70S and L79F; *** for K154E). Combined data from three independent experiments are shown. *** = <0.001; ** = <0.01 by unpaired, two-tailed Student's T test. Controls (HsIFNλ4-TT and EGFP) are not shown but gave zero protection.

E) Segment of an amino acid alignment (amino acids 151 to 157) of selected orthologues of HsIFNλ4 from different species as well as 2 human paralogues HsIFNλ1 and HsIFNλ3. At position 154, HsIFNλ4 encodes a lysine (K; blue) while sequences from all other species predict a glutamic acid at this position (E; red).

F) Antiviral activity of IFNλ from the different species indicated (human [Hs], chimpanzee [Pt] and macaque [Mm]) encoding an E (red bars) or K (black bars) at position 154 alongside the equivalent amino acid substitution in HsIFNλ3op in an anti-EMCV CPE assay relative to wt HsIFNλ4 in HepaRG cells. Order denotes wt then variant IFNλ. Data show +/- SD (n = 3 replicates) and are representative of two independent experiments. *** = <0.001; * = <0.05 by unpaired, two-tailed Student's T test.

G) IFN signalling reporter assay for mutant IFNλ4s from different species encoding an E (red lines) or K (black lines) at position 154 alongside the equivalent change in HsIFNλ3op. HsIFNλ4 = triangles; PtIFNλ4 = squares; MmIFNλ4 = stars; HsIFNλ3 = inverted triangles. Serial two-fold dilutions of CM (1:2 to 1:2097152) were incubated with an IFN reporter cell line (HepaRG.EGFP-ISG15). EGFP-positive cells (%) were measured by flow cytometry at each dilution. Data shown are +/- SEM (n = 3 replicates) and are representative of two independent experiments. Comparison of all E

versus K substituted forms of IFNλ4 within a homologue yielded significance values (p = <0.001 by Two-way ANOVA).

H) *MX1* gene expression by RT-qPCR for mutant IFNλ4s from different species encoding an E (red bars) or K (black bars) at position 154 alongside the equivalent change in HsIFNλ3op. Data represent the relative fold change of *MX1* by RT-qPCR in cells stimulated with CM (dilution 1:4) for 24 hrs compared to HsIFNλ4 wt. Data show +/- SEM (n = 6 replicates) combined from two independent experiments. *** = <0.001; ** = <0.01 by unpaired, two-tailed Student's T test.

Figure 2. K154E enhances antiviral activity of IFNλ4 but is very rarely found in the human population

A) Antiviral activity of HsIFNλ4 variants against HCVcc infection in Huh7 cells measured by RT-qPCR. HsIFNλ-containing CM (1:3) was incubated with Huh7 cells for 24 hrs before infection with HCVcc Jc1 (MOI = 0.01). HCV RNA was measured by RT-qPCR on RNA isolated at 72hpi. Results shown are relative to infection in cells treated with EGFP CM. Data show +/- SEM (n = 6 replicates) combined from two independent experiments. * = <0.05 by unpaired, two-tailed Student's T test.

B) The effect of HsIFNλ4 on JFH1 HCV pseudoparticle (pp) infectivity in Huh7 cells. Relative light units (RLU) in the media of luciferase-expressing MLV pseudoparticles following inoculation of Huh7 cells stimulated with CM (1:3), relative (%) to CM from EGFP-transfected cells. Luciferase activity was measured at 72 hrs after inoculation. Error bars show +/- SEM from experiments performed in triplicate. * = <0.05; ns = not significant by Student's T test.

C) The effect of HsIFNλ4 CM on transient HCV RNA replication using a subgenomic replicon assay in Huh7 cells. Huh7 cells were treated with CM (1:3) for 24 hrs before transfection with *in vitro* transcribed JFH1 HCV-SGR RNA expressing *Gaussia* luciferase. RLU secreted into the media was measured at 4, 24, 48 and 72 hpt. CM was obtained from cells transfected with EGFP (green), HsIFNλ4 wt (orange), HsIFNλ4 P70S (cyan), HsIFNλ4 L79F (yellow), HsIFNλ4 K154E (purple) and HsIFNλ3op (red). Error bars show +/- SD from experiments performed in triplicate. Data are representative of two independent experiments. *** = <0.001 by two-way ANOVA.

D) Violin plot of significant, differentially-expressed genes (log2 fold change compared to RNA from cells treated with EGFP CM 1:4 dilution) by RNA-Seq in A549 cells stimulated with different HsIFNλs for 24 hrs. CM was obtained from cells transfected with HsIFNλ3op (red); HsIFNλ4 wt (green); HsIFNλ4 P70S (cyan), and HsIFNλ4 K154E (purple).

E) Comparison of differentially-expressed genes (significant and at least 2-fold difference) stimulated by the HsIFNλ4 variants (HsIFNλ4 wt in green, HsIFNλ4 P70S in cyan and HsIFNλ4 K154E in purple) illustrated by a Venn diagram showing shared and unique genes. Three examples in overlapping and unique areas of the Venn diagram are highlighted.

F) Heat map of log2 fold change in RNA-Seq transcripts induced by the HsIFNλ4 variants from Figure 2D and 2E for chimpanzee-specific genes (n = 32) from Figure 1A.

G) Geographical location and frequency of HsIFNλ4 K154E in African hunter-gatherer genomes (Pygmy, n = 5 individuals, Sandawe (S) n = 5 individuals and Hadza (H) n = 5 individuals). Two Pygmy individuals within two tribes (Baka and

609 Bakola) were found to encode the HsIFNλ4 K154E variant. HsIFNλ4 genotype
610 and additional nonsynonymous variants detected are shown. Variants tested in our
611 functional screen with no significant effect on antiviral activity are indicated (*).
612 H) Presence of HsIFNλ4 E154 (purple) versus HsIFNλ4 K154 (green) on a
613 cladogram of human and chimpanzee evolution. Archaic human (Neanderthal and
614 Denisovan) as well as other basal human populations (San, Sandawe and Hadza)
615 only encode HsIFNλ4 K154. Earliest detection of the HsIFNλ4 TT frameshift and
616 activity-reducing HsIFNλ4 P70S and HsIFNλ4 L79F variants are shown.
617 I) Modelled structure of HsIFNλ4 showing position 154 at a central location in the
618 molecule with reference to receptor subunit-binding interfaces (IFNλR1 and
619 IL10R2). Overlapping crystal structures for HsIFNλ1 (green) and HsIFNλ3 (dark
620 blue) are overlaid together with a homology model for HsIFNλ4 (*, light blue). In
621 the overlapping structures, the homologous position for HsIFNλ4 E154 makes
622 intramolecular non-covalent interactions with two distinct regions within IFNλ.
623
624 **Figure S1.**
625 A) Ancestry-based localization and frequency of human non-synonymous variants of
626 HsIFNλ4 in African (AFR), South Asian (SAS), East Asian (EAS), European
627 (EUR) and American (AMR) populations within the 1000 Genomes dataset. 'n'
628 represents the number of alleles tested in each population. Common and rare
629 variants are those which have frequencies of >1% and <1% respectively in the
630 1000 Genome data. Common variants include: wt (orange), C17Y (light green),
631 R60P (dark green) and P70S (cyan). Rare variants (purple) include: A8S, C17R,
632 R25Q, S56R, P73S, L79F, K133M, V134A, R151P, K154E, S156N, V158I.
633 Variants K133M and S156N (black) did not have ethnicity associated with them

but were found in the dataset from the Netherlands (Genome of the Netherlands cohort).

B) *MX1* gene expression determined by RT-qPCR following stimulation of cells with HsIFNλ4 variants. Relative fold change of genes in HepaRG cells stimulated with CM from plasmid-transfected cells compared to CM from mock-transfected cells (1:4) for 24 hrs. Additional HsIFNλ4 variants are shown as controls (the frameshift HsIFNλ4 TT, a non-natural non-glycosylated HsIFNλ4 N61A variant as well as HsIFNλ4 F159A and HsIFNλ4 L162A [both of which are predicted to reduce interaction with the IFNλR1 receptor subunit and hence lower activity based on (Gad et al. 2009). Data are shown relative to mock-stimulated cells. Data shown are +/- SEM (n = 3).

C) Representative blot showing production of intracellular HsIFNλ4 variants by Western blot analysis of lysates from plasmid-transfected producer HEK293T cells as measured with an anti-FLAG ('F') primary antibody. Tubulin ('T') was used as a loading control. Cells either mock-transfected, transfected with an irrelevant plasmid (EGFP) or transfected with the frameshift IFNλ4 TT variant were used as negative controls. Upper (glycosylated; G) and lower (non-glycosylated; NG) forms of HsIFNλ4 are highlighted. A non-specific band in the EGFP-transfected extract is shown (*).

D) Quantification of intracellular glycosylated (green) and non-glycosylated (blue) HsIFNλ4 variants by Western blot analysis of lysates from plasmid-transfected producer HEK293T cells. Data shown are +/- SEM combined from three independent experiments.

E) Comparative functional activity of intracellular and cell-released HsIFNL4 wt (WT) and the HsIFNλ4 K154E variant in the EMCV antiviral assay. Cells were

either directly lysed (0 washes) or washed with PBS (3x washes) after removal of CM. Data for CM (supt) and cell lysates (lys) are shown.

F) Production of intracellular IFNλ4 from different species encoding E or K at position 154 alongside the equivalent change in HsIFNλ3op by Western blot analysis of lysates from plasmid-transfected producer HEK293T cells. The IFNλ4 variants were detected with an anti-FLAG antibody ('F'). Tubulin ('T') was used as a loading control. Mock- and EGFP-transfected cells were used as negative controls.

Figure S2.

A) Antiviral activity of HsIFNλ4 wt and HsIFNλ4 variants against HCVcc infection in Huh7 cells by determining virus antigen-positive cells (HCV NS5A protein). CM containing HsIFNλ3op and HsIFNλ4 wt and variants (1:3) was incubated with Huh7 cells for 24 hrs before infection with HCVcc Jc1 (MOI = 0.01 $TCID_{50}$/cell). HCVcc RNA was measured by RT-qPCR on total RNA isolated at 72hpi. Results are shown relative to infection in cells treated with CM from EGFP-transfected cells. Error bars for HCVcc RNA show +/- SEM from 6 replicates.

B) Effect of HsIFNλ4 wt and variants on entry of MLV pseudoparticles (pp) that lack HCV E1E2 (MLV core particles) in Huh7 cells. Following inoculation of Huh7 cells stimulated with CM (1:3). Luciferase activity was measured at 72hpi. Error bars show +/- SEM from experiments performed in triplicate. *** = <0.001 by unpaired, two-tailed Student's T test.

C) The effect of HsIFNλ4 wt and variants on translation of a non-replicative JFH1 HCV-SGR (GND) in Huh7 cells. Huh7 cells were treated with CM (1:3) for 24

hrs before transfection with *in vitro* transcribed JFH1 HCV-SGR (GND) RNA. RLU secreted into the media was measured at 4, 24, 48 and 72 hpt. Error bars show +/- SD from experiments performed in triplicate. Data are representative of two independent experiments.

D) Antiviral activity of HsIFNλ4 wt and variants on IAV (WSN strain) infection in A549 cells as determined by plaque assay of virus released from infected cells at 48hpi. HsIFNλ4- and EGFP-containing CM (1:3) was incubated with A549 cells for 24 hrs before infection with IAV strain (MOI = 0.01 PFU/cell). Supernatant was harvested and titrated on MDCK cells. Error bars show +/- SEM in triplicate. * = <0.05 by unpaired, two-tailed Student's T test.

E) Antiviral activity of HsIFNλ4 wt and variants on ZIKV (strain PE243) infection in A549 cells as determined by plaque assay of virus released from infected cells at 72hpi. HsIFNλ4- and EGFP-containing CM (1:3) was incubated with A549 cells for 24 hrs before infection with ZIKV (MOI = 0.01). Supernatant was harvested at 72hpi and infectivity was titrated on Vero cells. Error bars show +/- SEM in triplicate * = <0.05 by unpaired, two-tailed Student's T test.

F) Number of significantly differentially-expressed genes in each experimental condition (sample 1) relative to each other condition (sample 2). Colour shaded by number of transcripts shared, as shown.

G) Heat map of all significantly differentially-expressed genes (log10 Fragments Per Kilobase of transcript per Million mapped reads (FKPM) in each experimental condition including EGFP CM-stimulated cells.

H) Pathway analysis using IPA on all significantly differentially-expressed genes (>2 fold). The top five most significantly induced pathways are shown [-log(p value)].

I) Modelled structure of HsIFNλ4 showing position 79 or the homologous position with reference to receptor subunit-binding interfaces (IFNλR1 and IL10R2). Shown overlapping are the crystal structures for HsIFNλ1 (green) and HsIFNλ3 (dark blue) overlaid together with a homology model (*) of HsIFNλ4 (light blue).

REFERENCES

Bassett, S. E., K. M. Brasky, and R. E. Lanford. 1998. Analysis of hepatitis C virus-inoculated chimpanzees reveals unexpected clinical profiles. Journal of Virology 72:2589–2599.

Bigger, C. B., K. M. Brasky, and E. Robert. 2001. DNA microarray analysis of chimpanzee liver during acute resolving hepatitis c virus infection dna microarray analysis of chimpanzee liver during acute resolving hepatitis C virus infection. Journal of Virology 75:7059–7065.

Blazek, K., H. L. Eames, M. Weiss, A. J. Byrne, D. Perocheau, J. E. Pease, S. Doyle, F. McCann, R. O. Williams, and I. A. Udalova. 2015. IFN-λ resolves inflammation via suppression of neutrophil infiltration and IL-1β production. The Journal of Experimental Medicine 212:845–853.

Boldanova, T., A. Suslov, M. H. Heim, and A. Necsulea. 2017. Transcriptional response to hepatitis C virus infection and interferon-alpha treatment in the human liver. EMBO Molecular Medicine 9:816–834.

Bukh, J. 2004. A critical role for the chimpanzee model in the study of hepatitis C. Hepatology 39:1469–1475.

Cohen, T. S., and A. S. Prince. 2013. Bacterial Pathogens Activate a Common Inflammatory Pathway through IFNλ Regulation of PDCD4. PLoS Pathogens 9:e1003682.

Cowton, V. M., A. G. N. Angus, S. J. Cole, C. K. Markopoulou, A. Owsianka, J. I. Dunlop, D. E. Gardner, T. Krey, and A. H. Patel. 2016. Role of conserved E2 residue W420 in receptor binding and hepatitis C virus infection. Journal of Virology 90:7456–7468.

Dill, M. T., Z. Makowska, F. H. T. Duong, F. Merkofer, M. Filipowicz, T. F. Baumert, L. Tornillo, L. Terracciano, and M. H. Heim. 2012. Interferon-γ–stimulated genes, but not USP18, are expressed in livers of patients with acute hepatitis C. Gastroenterology

143:777–786.e6.

Dixit, E., S. Boulant, Y. Zhang, A. S. Y. Lee, C. Odendall, B. Shum, N. Hacohen, Z. J. Chen, S. P. Whelan, M. Fransen, M. L. Nibert, G. Superti-Furga, and J. C. Kagan. 2010. Peroxisomes are signaling platforms for antiviral innate immunity. Cell 141:668–681.

Domingues, P., C. G. G. Bamford, C. Boutell, and J. McLauchlan. 2015. Inhibition of hepatitis C virus RNA replication by ISG15 does not require its conjugation to protein substrates by the HERC5 E3 ligase. Journal of General Virology 96: 3236-3242.

Donald, C. L., B. Brennan, S. L. Cumberworth, V. V. Rezelj, J. J. Clark, M. T. Cordeiro, R. Freitas de Oliveira França, L. J. Pena, G. S. Wilkie, A. Da Silva Filipe, C. Davis, J. Hughes, M. Varjak, M. Selinger, L. Zuvanov, A. M. Owsianka, A. H. Patel, J. McLauchlan, B. D. Lindenbach, G. Fall, A. A. Sall, R. Biek, J. Rehwinkel, E. Schnettler, and A. Kohl. 2016. Full genome sequence and sfRNA interferon antagonist activity of Zika virus from Recife, Brazil. PLoS Neglected Tropical Diseases 10:e0005048.

Eslam, M., A. M. Hashem, R. Leung, M. Romero-Gomez, T. Berg, G. J. Dore, H. L. K. Chan, W. L. Irving, D. Sheridan, M. L. Abate, L. A. Adams, A. Mangia, M. Weltman, E. Bugianesi, U. Spengler, O. Shaker, J. Fischer, L. Mollison, W. Cheng, E. Powell, J. Nattermann, S. Riordan, D. McLeod, N. J. Armstrong, M. W. Douglas, C. Liddle, D. R. Booth, J. George, G. Ahlenstiel, J. Ampuero, M. Bassendine, V. W. S. Wong, C. Rosso, R. White, L. Mezzabotta, V. Suppiah, M. Michalk, B. Malik, G. Matthews, T. Applegate, J. Grebely, V. Fragomeli, J. R. Jonsson, and R. Santaro. 2015. Interferon-λ rs12979860 genotype and liver fibrosis in viral and non-viral chronic liver disease. Nature Communications 6:6422.

Espinosa, V., O. Dutta, C. McElrath, P. Du, Y.-J. Chang, B. Cicciarelli, A. Pitler, I. Whitehead, J. J. Obar, J. E. Durbin, S. V. Kotenko, and A. Rivera. 2017. Type III

763 interferon is a critical regulator of innate antifungal immunity. Science Immunology
764 2:eaan5357.
765 Fan, W., S. Xie, X. Zhao, N. Li, C. Chang, L. Li, G. Yu, X. Chi, Y. Pan, J. Niu, J. Zhong, and
766 B. Sun. 2016. IFN-λ4 desensitizes the response to IFN-α treatment in chronic hepatitis C
767 through long-term induction of USP18. Journal of General Virology 97:2210–2220.
768 Foupouapouognigni, Y., S. A. Sadeuh Mba, E. B. a Betsem, D. Rousset, A. Froment, A.
769 Gessain, and R. Njouom. 2011. Hepatitis B and C virus infections in the three Pygmy
770 groups in Cameroon. Journal of Clinical Microbiology 49:737–740.
771 Gad, H. H., C. Dellgren, O. J. Hamming, S. Vends, S. R. Paludan, and R. Hartmann. 2009.
772 Interferon-λ is functionally an interferon but structurally related to the interleukin-10
773 family. Journal of Biological Chemistry 284:20869–20875.
774 Galani, I. E., V. Triantafyllia, E.-E. Eleminiadou, O. Koltsida, A. Stavropoulos, M.
775 Manioudaki, D. Thanos, S. E. Doyle, S. V. Kotenko, K. Thanopoulou, and E.
776 Andreakos. 2017. Interferon-λ mediates non-redundant front-line antiviral protection
777 against influenza virus infection without compromising host fitness. Immunity 46:875–
778 890.e6.
779 Ge, D., J. Fellay, A. J. Thompson, J. S. Simon, K. V. Shianna, T. J. Urban, E. L. Heinzen, P.
780 Qiu, A. H. Bertelsen, A. J. Muir, M. Sulkowski, J. G. McHutchison, and D. B.
781 Goldstein. 2009. Genetic variation in IL28B predicts hepatitis C treatment-induced viral
782 clearance. Nature 461:399–401.
783 Hamming, O. J., E. Terczyńska-Dyla, G. Vieyres, R. Dijkman, S. E. Jørgensen, H. Akhtar, P.
784 Siupka, T. Pietschmann, V. Thiel, and R. Hartmann. 2013. Interferon lambda 4 signals
785 via the IFNλ receptor to regulate antiviral activity against HCV and coronaviruses. The
786 EMBO Journal 32:3055–3065.
787 Jones, D. M., P. Domingues, P. Targett-Adams, and J. McLauchlan. 2010. Comparison of

788 U2OS and Huh-7 cells for identifying host factors that affect hepatitis C virus RNA
789 replication. Journal of General Virology 91:2238–2248.
790 Key, F. M., B. Peter, M. Y. Dennis, E. Huerta-Sánchez, W. Tang, L. Prokunina-Olsson, R.
791 Nielsen, and A. M. Andrés. 2014. Selection on a variant associated with improved viral
792 clearance drives local, adaptive pseudogenization of interferon lambda 4 (IFNL4). PLoS
793 Genetics 10:e1004681.
794 Lachance, J., B. Vernot, C. C. Elbers, B. Ferwerda, A. Froment, J.-M. Bodo, G. Lema, W.
795 Fu, T. B. Nyambo, T. R. Rebbeck, K. Zhang, J. M. Akey, and S. A. Tishkoff. 2012.
796 Evolutionary history and adaptation from high-coverage whole-genome sequences of
797 diverse African hunter-gatherers. Cell 150:457–469.
798 Lanford, R. E., B. Guerra, C. B. Bigger, H. Lee, D. Chavez, and K. M. Brasky. 2007. Lack of
799 response to exogenous interferon-α in the liver of chimpanzees chronically infected with
800 hepatitis C virus. Hepatology 46:999–1008.
801 Lazear, H. M., B. P. Daniels, A. K. Pinto, A. C. Huang, S. C. Vick, S. E. Doyle, M. Gale, R.
802 S. Klein, and M. S. Diamond. 2015a. Interferon-λ restricts West Nile virus
803 neuroinvasion by tightening the blood-brain barrier. Science Translational Medicine
804 7:284ra59-284ra59.
805 Lazear, H. M., T. J. Nice, and M. S. Diamond. 2015b. Interferon-λ: immune functions at
806 barrier surfaces and beyond. Immunity 43:15–28.
807 Lindenbach, B. D., M. J. Evans, A. J. Syder, B. Wölk, T. L. Tellinghuisen, C. C. Liu, T.
808 Maruyama, R. O. Hynes, D. R. Burton, J. a McKeating, and C. M. Rice. 2005. Complete
809 replication of hepatitis C virus in cell culture. Science. 309:623–626.
810 Mallick, S., H. Li, M. Lipson, I. Mathieson, M. Gymrek, F. Racimo, M. Zhao, N. Chennagiri,
811 S. Nordenfelt, A. Tandon, P. Skoglund, I. Lazaridis, S. Sankararaman, Q. Fu, N.
812 Rohland, G. Renaud, Y. Erlich, T. Willems, C. Gallo, J. P. Spence, Y. S. Song, G.

Poletti, F. Balloux, G. van Driem, P. de Knijff, I. G. Romero, A. R. Jha, D. M. Behar, C. M. Bravi, C. Capelli, T. Hervig, A. Moreno-Estrada, O. L. Posukh, E. Balanovska, O. Balanovsky, S. Karachanak-Yankova, H. Sahakyan, D. Toncheva, L. Yepiskoposyan, C. Tyler-Smith, Y. Xue, M. S. Abdullah, A. Ruiz-Linares, C. M. Beall, A. Di Rienzo, C. Jeong, E. B. Starikovskaya, E. Metspalu, J. Parik, R. Villems, B. M. Henn, U. Hodoglugil, R. Mahley, A. Sajantila, G. Stamatoyannopoulos, J. T. S. Wee, R. Khusainova, E. Khusnutdinova, S. Litvinov, G. Ayodo, D. Comas, M. F. Hammer, T. Kivisild, W. Klitz, C. A. Winkler, D. Labuda, M. Bamshad, L. B. Jorde, S. A. Tishkoff, W. S. Watkins, M. Metspalu, S. Dryomov, R. Sukernik, L. Singh, K. Thangaraj, S. Pääbo, J. Kelso, N. Patterson, and D. Reich. 2016. The Simons Genome Diversity Project: 300 genomes from 142 diverse populations. Nature 538:201–206.

Manry, J., G. Laval, E. Patin, S. Fornarino, Y. Itan, M. Fumagalli, M. Sironi, M. Tichit, C. Bouchier, J.-L. Casanova, L. B. Barreiro, and L. Quintana-Murci. 2011. Evolutionary genetic dissection of human interferons. The Journal of Experimental Medicine 208:2747–2759.

Mendoza, J. L., W. M. Schneider, H.-H. Hoffmann, K. Vercauteren, K. M. Jude, A. Xiong, I. Moraga, T. M. Horton, J. S. Glenn, Y. P. de Jong, C. M. Rice, and K. C. Garcia. 2017. The IFN-λ-IFN-λR1-IL-10Rβ complex reveals structural features underlying type III IFN functional plasticity. Immunity 46:379–392.

Miknis, Z. J., E. Magracheva, W. Li, A. Zdanov, S. V. Kotenko, and A. Wlodawer. 2010. Crystal structure of Human interferon-λ1 in complex with its high-affinity receptor interferon-λR1. Journal of Molecular Biology 404:650–664.

Mohamed, M., A. McLees, and R. M. Elliott. 2009. Viruses in the Anopheles A, Anopheles B, and Tete serogroups in the Orthobunyavirus genus (family Bunyaviridae) do not encode an NSs protein. Journal of Virology 83:7612–7618.

838 Mulangu, S., M. Borchert, J. Paweska, A. Tshomba, A. Afounde, A. Kulidri, R. Swanepoel,
839 J.-J. Muyembe-Tamfum, and P. Van der Stuyft. 2016. High prevalence of IgG
840 antibodies to Ebola virus in the Efé pygmy population in the Watsa region, Democratic
841 Republic of the Congo. BMC Infectious Diseases 16:263.
842 Nanda, S., M. B. Havert, G. M. Calderón, M. Thomson, C. Jacobson, D. Kastner, and T. J.
843 Liang. 2008. Hepatic transcriptome analysis of hepatitis C virus infection in
844 chimpanzees defines unique gene expression patterns associated with viral clearance.
845 PLoS ONE 3:e3442.
846 Nice, T. J., M. T. Baldridge, B. T. McCune, J. M. Norman, H. M. Lazear, M. Artyomov, M.
847 S. Diamond, and H. W. Virgin. 2015. Interferon-λ cures persistent murine norovirus
848 infection in the absence of adaptive immunity. Science 347:269–273.
849 Njouom, R., C. Pasquier, A. Ayouba, A. Gessain, A. Froment, J. Mfoupouendoun, R.
850 Pouillot, M. Dubois, K. Sandres-Sauné, J. Thonnon, J. Izopet, and E. Nerrienet. 2003.
851 High rate of hepatitis C virus infection and predominance of genotype 4 among elderly
852 inhabitants of a remote village of the rain forest of South Cameroon. Journal of Medical
853 Virology 71:219–225.
854 Odendall, C., A. A. Voak, and J. C. Kagan. 2017. Type III IFNs are commonly induced by
855 bacteria-sensing TLRs and reinforce epithelial barriers during infection. The Journal of
856 Immunology:ji1700250.
857 Park, H., E. Serti, O. Eke, Muchmore B, Prokunina-Olsson L, Capone S, Folgori A,
858 Rehermann B. 2012. IL-29 is the dominant type III interferon produced by hepatocytes
859 during acute hepatitis C virus infection. Hepatology. 56:2060–2070.
860 Pietschmann, T., A. Kaul, G. Koutsoudakis, A. Shavinskaya, S. Kallis, E. Steinmann, K.
861 Abid, F. Negro, M. Dreux, F.-L. Cosset, and R. Bartenschlager. 2006. Construction and
862 characterization of infectious intragenotypic and intergenotypic hepatitis C virus

chimeras. Proceedings of the National Academy of Sciences 103:7408–7413.

Prokunina-Olsson, L., B. Muchmore, W. Tang, R. M. Pfeiffer, H. Park, H. Dickensheets, D. Hergott, P. Porter-Gill, A. Mumy, I. Kohaar, S. Chen, N. Brand, M. Tarway, L. Liu, F. Sheikh, J. Astemborski, H. L. Bonkovsky, B. R. Edlin, C. D. Howell, T. R. Morgan, D. L. Thomas, B. Rehermann, R. P. Donnelly, and T. R. O'Brien. 2013. A variant upstream of IFNL3 (IL28B) creating a new interferon gene IFNL4 is associated with impaired clearance of hepatitis C virus. Nature Genetics 45:164–171.

Ran, F. A., P. D. Hsu, J. Wright, V. Agarwala, D. A. Scott, and F. Zhang. 2013. Genome engineering using the CRISPR-Cas9 system. Nature Protocols 8:2281–2308.

Randall, R. E., and S. Goodbourn. 2008. Interferons and viruses: an interplay between induction , signalling , antiviral responses and virus countermeasures. Journal of General Virology 89:1–47.

Ray, S. C., Q. Mao, R. E. Lanford, S. Bassett, O. Laeyendecker, Y. M. Wang, and D. L. Thomas. 2000. Hypervariable region 1 sequence stability during hepatitis C virus replication in chimpanzees. Journal of Virology 74:3058–66.

Schoggins, J. W. 2014. Interferon-stimulated genes: roles in viral pathogenesis. Current Opinion in Virology 6C:40–46.

Schoggins, J. W., S. J. Wilson, M. Panis, M. Y. Murphy, C. T. Jones, P. Bieniasz, and C. M. Rice. 2011. A diverse range of gene products are effectors of the type I interferon antiviral response. Nature 472:481–485.

Sheahan, T., N. Imanaka, S. Marukian, M. Dorner, P. Liu, A. Ploss, and C. M. Rice. 2014. Interferon lambda alleles predict innate antiviral immune responses and hepatitis C virus permissiveness. Cell Host & Microbe 15:190–202.

Su, A. I., J. P. Pezacki, L. Wodicka, A. D. Brideau, L. Supekova, R. Thimme, S. Wieland, J. Bukh, R. H. Purcell, P. G. Schultz, and F. V. Chisari. 2002. Genomic analysis of the

888 host response to hepatitis C virus infection. Proceedings of the National Academy of
889 Sciences 99:15669–15674.
890 Terczyńska-Dyla, E., S. Bibert, F. H. T. Duong, I. Krol, S. Jørgensen, E. Collinet, Z. Kutalik,
891 V. Aubert, A. Cerny, L. Kaiser, R. Malinverni, A. Mangia, D. Moradpour, B. Müllhaupt,
892 F. Negro, R. Santoro, D. Semela, N. Semmo, L. Rubbia-Brandt, G. Martinetti, M.
893 Gorgievski, J.-F. Dufour, H. Hirsch, B. Helbling, S. Regenass, G. Dollenmaier, G.
894 Cathomas, M. H. Heim, P.-Y. Bochud, and R. Hartmann. 2014. Reduced IFNλ4 activity
895 is associated with improved HCV clearance and reduced expression of interferon-
896 stimulated genes. Nature Communications 5:5699.
897 Thimme, R., J. Bukh, H. C. Spangenberg, S. Wieland, J. Pemberton, C. Steiger, S.
898 Govindarajan, R. H. Purcell, and F. V. Chisari. 2002. Viral and immunological
899 determinants of hepatitis C virus clearance, persistence, and disease. Proceedings of the
900 National Academy of Sciences 99:15661–15668.
901 Thomas, E., V. D. Gonzalez, Q. Li, A. A. Modi, W. Chen, M. Noureddin, Y. Rotman, and T.
902 J. Liang. 2012. HCV infection induces a unique hepatic innate immune response
903 associated with robust production of type III interferons. Gastroenterology 142:978–988.
904 Trapnell, C., A. Roberts, L. Goff, G. Pertea, D. Kim, D. R. Kelley, H. Pimentel, S. L.
905 Salzberg, J. L. Rinn, and L. Pachter. 2012. Differential gene and transcript expression
906 analysis of RNA-seq experiments with TopHat and Cufflinks. Nature Protocols 7:562–
907 578.
908 Walker, C. M. 1997. Comparative features of hepatitis C virus infection in humans and
909 chimpanzees. Springer Seminars in Immunopathology 19:85–98.
910 Yu, C., D. Boon, S. L. McDonald, T. G. Myers, K. Tomioka, H. Nguyen, R. E. Engle, S.
911 Govindarajan, S. U. Emerson, and R. H. Purcell. 2010. Pathogenesis of hepatitis E Virus
912 and hepatitis C virus in chimpanzees: similarities and differences. Journal of Virology

913 84:11264–11278.

FIGURE 1

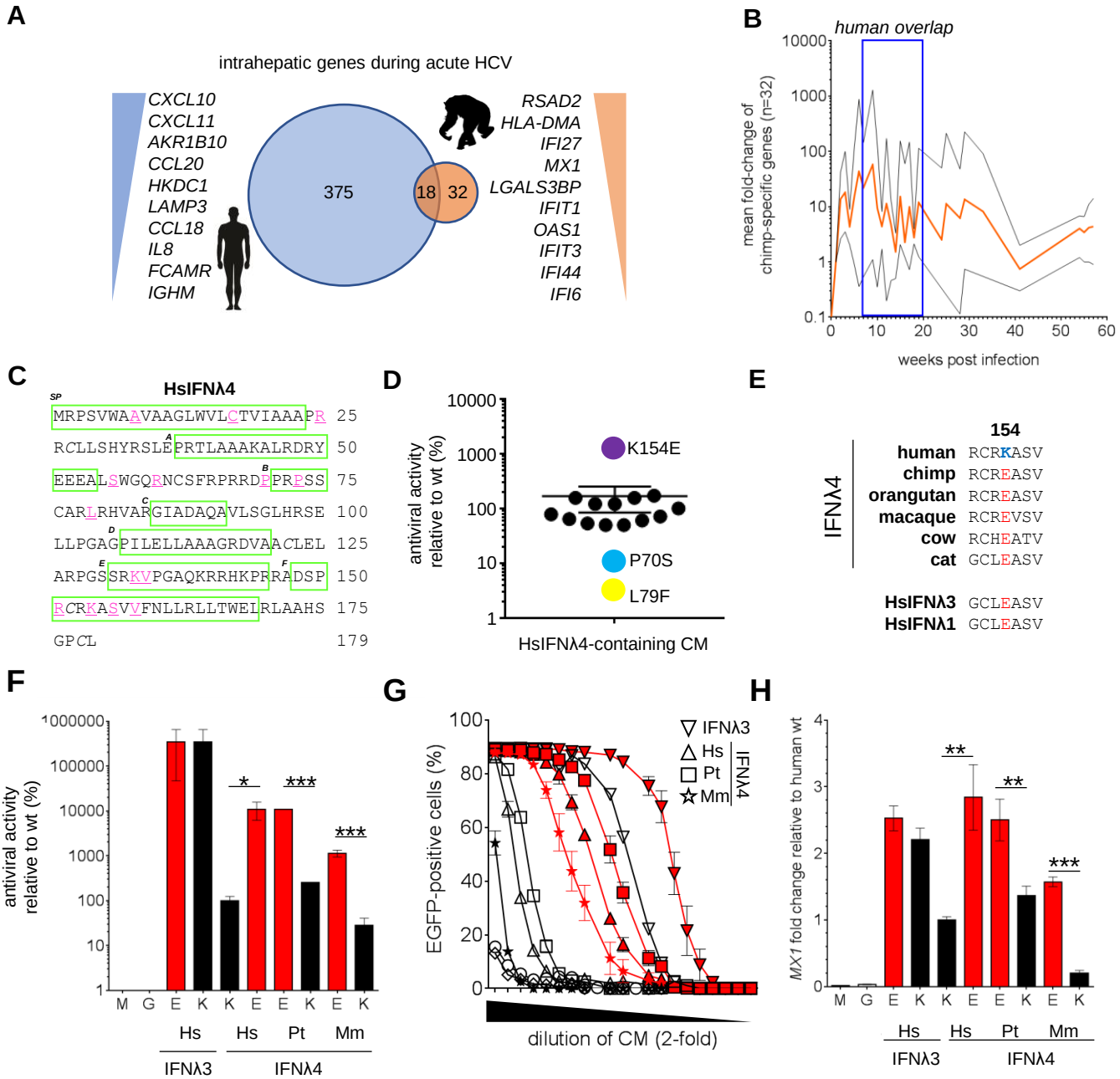
A
intrahepatic genes during acute HCV
CXCL10
CXCL11
AKR1B10
CCL20
HKDC1
LAMP3
CCL18
IL8
FCAMR
IGHM
375
18
32
RSAD2
HLA-DMA
IFI27
MX1
LGALS3BP
IFIT1
OAS1
IFIT3
IFI44
IFI6
B
human overlap
mean fold-change of chimp-specific genes (n=32)
weeks post infection
C
HsIFNλ4
MRPSVWAAVAAGLWVLCTVIAAAPR 25
RCLLSHYRSLEPRTLAAAKALRDRY 50
EEEALSWGQRNCSFRPRRDPPRPSS 75
CARLRHVARGIADAQAVLSGLHRSE 100
LLPGAGPILELLAAAGRDVAACLEL 125
ARPGSSRKVPGAQKRRHKPRRADSP 150
RCRKASVVFNLLRLLTWELRLAAHS 175
GPCL 179
D
antiviral activity relative to wt (%)
K154E
P70S
L79F
HsIFNλ4-containing CM
E
IFNλ4
154
human RCRKASV
chimp RCREASV
orangutan RCREASV
macaque RCREVSV
cow RCHEATV
cat GCLEASV
HsIFNλ3 GCLEASV
HsIFNλ1 GCLEASV
F
antiviral activity relative to wt (%)
M G E K K E E K E K
Hs Hs Pt Mm
IFNλ3 IFNλ4
G
EGFP-positive cells (%)
IFNλ3
Hs
Pt
Mm
IFNλ4
dilution of CM (2-fold)
H
MX1 fold change relative to human wt
M G E K K E E K E K
Hs Hs Pt Mm
IFNλ3 IFNλ4

FIGURE 2

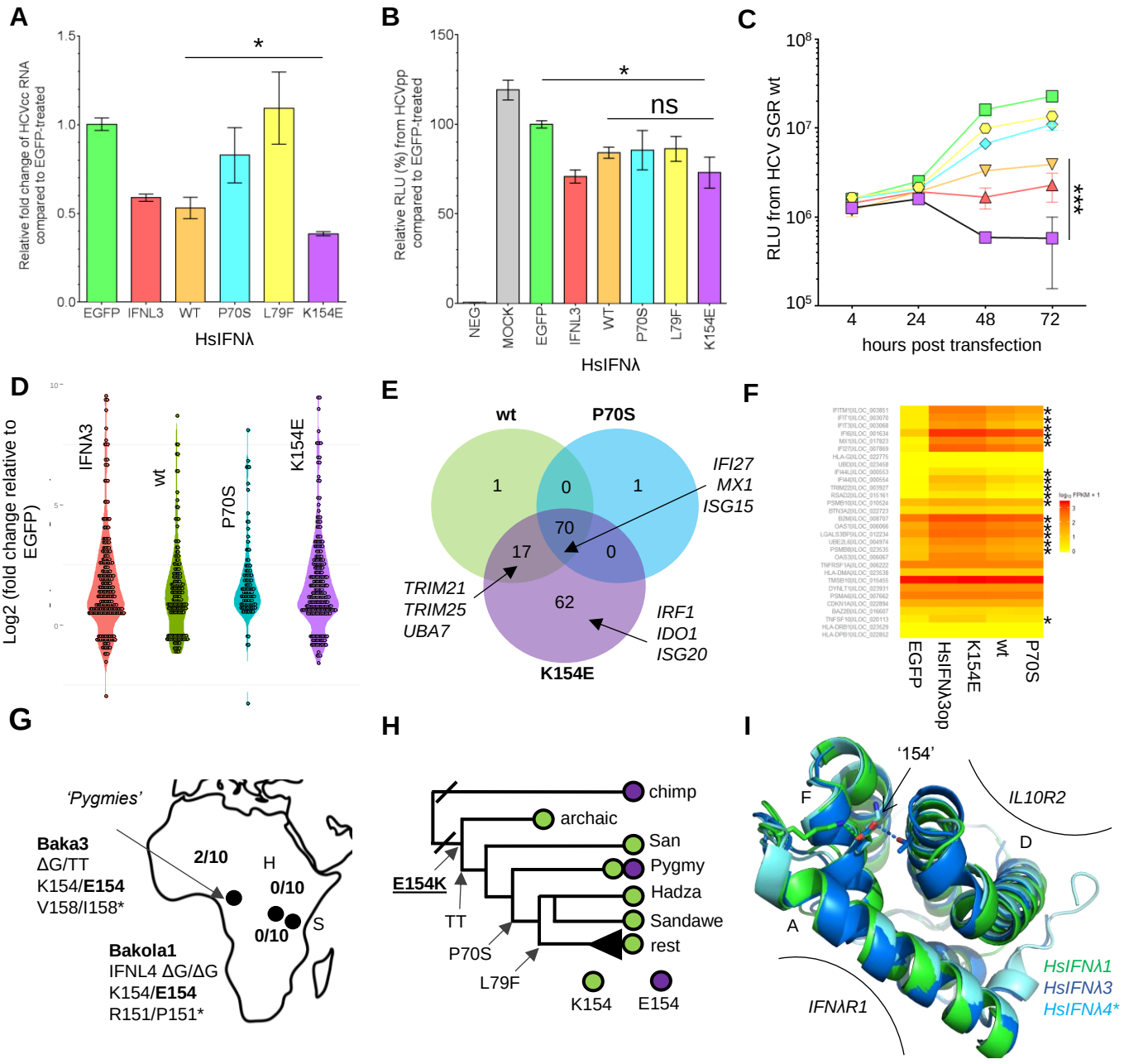
A
Relative fold change of HCVcc RNA compared to EGFP-treated
1.5
1.0
0.5
0.0
*
EGFP IFNL3 WT P70S L79F K154E
HsIFNλ
B
Relative RLU (%) from HCVpp compared to EGFP-treated
150
100
50
0
*
ns
NEG MOCK EGFP IFNL3 WT P70S L79F K154E
HsIFNλ
C
RLU from HCV SGR wt
10^8
10^7
10^6
10^5
***
4 24 48 72
hours post transfection
D
Log2 (fold change relative to EGFP)
IFNλ3
wt
P70S
K154E
E
wt
P70S
K154E
1
0
1
70
17
0
62
IFI27
MX1
ISG15
TRIM21
TRIM25
UBA7
IRF1
IDO1
ISG20
F
EGFP
HsIFNλ3op
K154E
wt
P70S
G
'Pygmies'
Baka3
ΔG/TT
K154/E154
V158/I158*
2/10
H
0/10
0/10
S
Bakola1
IFNL4 ΔG/ΔG
K154/E154
R151/P151*
H
chimp
archaic
San
Pygmy
Hadza
Sandawe
rest
E154K
TT
P70S
L79F
K154
E154
I
'154'
F
IL10R2
D
A
IFNλR1
HsIFNλ1
HsIFNλ3
HsIFNλ4*

FIGURE S1

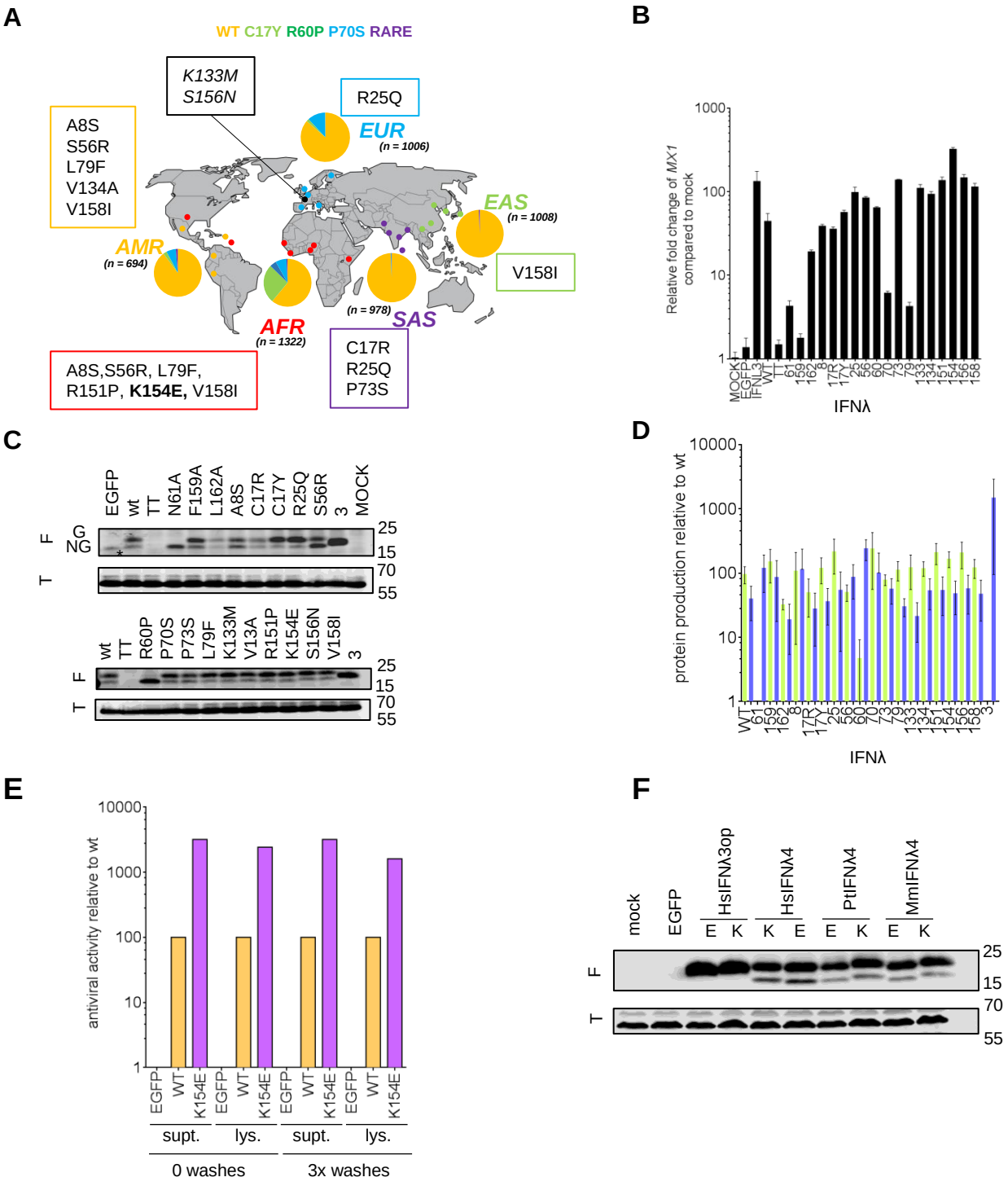
A
WT C17Y R60P P70S RARE
K133M
S156N
R25Q
A8S
S56R
L79F
V134A
V158I
EUR
(n = 1006)
EAS
(n = 1008)
AMR
(n = 694)
V158I
(n = 978)
SAS
AFR
(n = 1322)
A8S,S56R, L79F,
R151P, K154E, V158I
C17R
R25Q
P73S
B
Relative fold change of MX1
compared to mock
IFNλ
C
EGFP
wt
TT
N61A
F159A
L162A
A8S
C17R
C17Y
R25Q
S56R
3
MOCK
F
G
NG
T
25
15
70
55
wt
TT
R60P
P70S
P73S
L79F
K133M
V13A
R151P
K154E
S156N
V158I
3
D
protein production relative to wt
IFNλ
E
antiviral activity relative to wt
EGFP
WT
K154E
supt.
lys.
0 washes
3x washes
F
mock
EGFP
HsIFNλ3op
HsIFNλ4
PtIFNλ4
MmIFNλ4
E
K
F
T
25
15
70
55

FIGURE S2

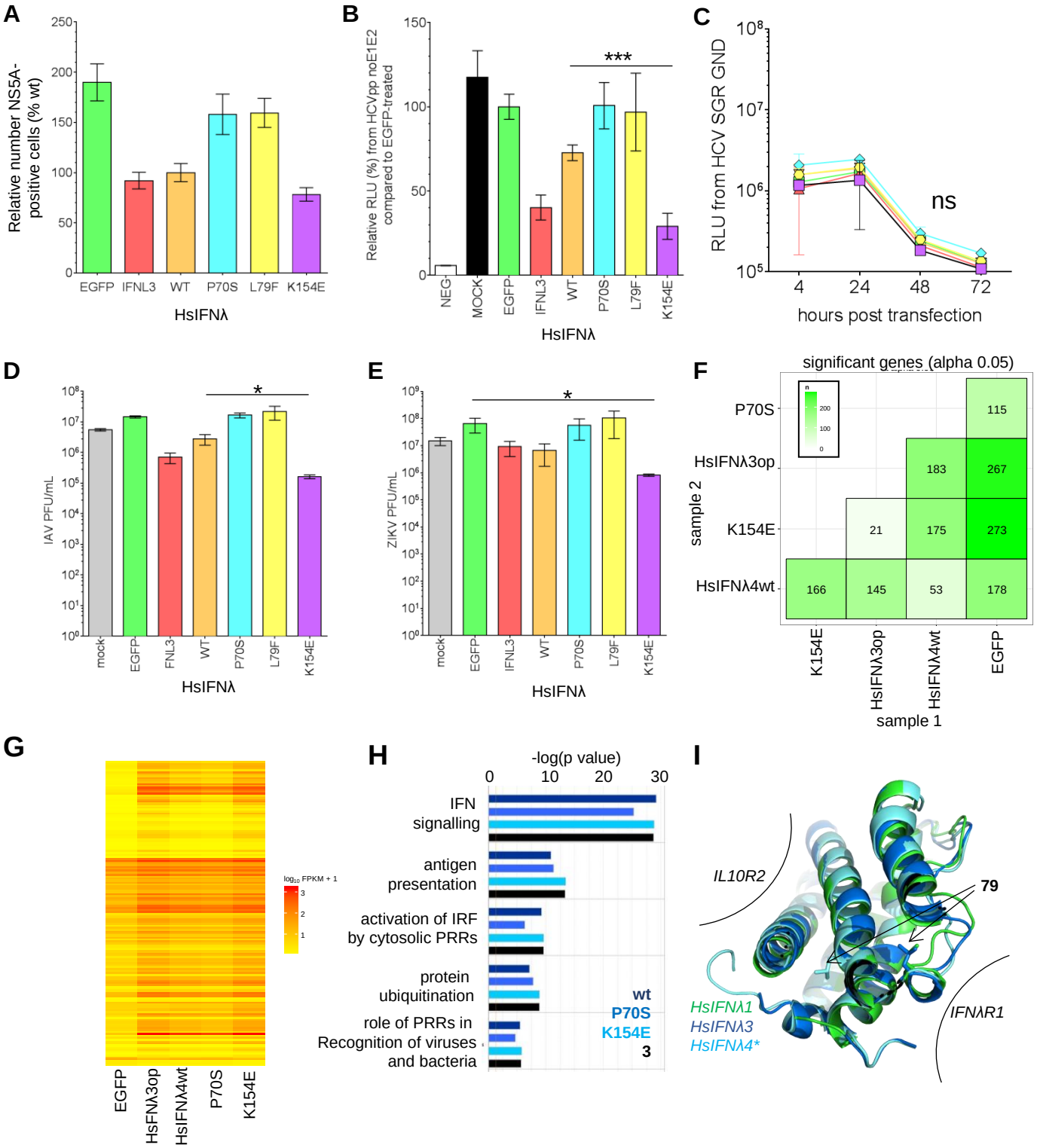
A
Relative number NS5A-positive cells (% wt)
EGFP IFNL3 WT P70S L79F K154E
HsIFNλ
B
Relative RLU (%) from HCVpp noE1E2 compared to EGFP-treated
***
NEG MOCK EGFP IFNL3 WT P70S L79F K154E
HsIFNλ
C
RLU from HCV SGR GND
ns
hours post transfection
D
IAV PFU/mL
*
mock EGFP FNL3 WT P70S L79F K154E
HsIFNλ
E
ZIKV PFU/mL
*
mock EGFP IFNL3 WT P70S L79F K154E
HsIFNλ
F
significant genes (alpha 0.05)
P70S
HsIFNλ3op
K154E
HsIFNλ4wt
sample 2
115
183 267
21 175 273
166 145 53 178
K154E HsIFNλ3op HsIFNλ4wt EGFP
sample 1
G
log10 FPKM + 1
EGFP HsFNλ3op HsIFNλ4wt P70S K154E
H
-log(p value)
IFN signalling
antigen presentation
activation of IRF by cytosolic PRRs
protein ubiquitination
role of PRRs in Recognition of viruses and bacteria
wt
P70S
K154E
I
IL10R2
79
HsIFNλ1
HsIFNλ3
HsIFNλ4*
IFNλR1